



**HAL**  
open science

## Influence of model parameter variability on the directivity filters of compact loudspeaker arrays

Alexander Mattioli Pasqual, Marc Pachebat, Philippe Herzog

► **To cite this version:**

Alexander Mattioli Pasqual, Marc Pachebat, Philippe Herzog. Influence of model parameter variability on the directivity filters of compact loudspeaker arrays. *Acoustics 2012*, Apr 2012, Nantes, France. pp.2839-2844. hal-00759534

**HAL Id: hal-00759534**

**<https://hal.science/hal-00759534>**

Submitted on 30 Nov 2012

**HAL** is a multi-disciplinary open access archive for the deposit and dissemination of scientific research documents, whether they are published or not. The documents may come from teaching and research institutions in France or abroad, or from public or private research centers.

L'archive ouverte pluridisciplinaire **HAL**, est destinée au dépôt et à la diffusion de documents scientifiques de niveau recherche, publiés ou non, émanant des établissements d'enseignement et de recherche français ou étrangers, des laboratoires publics ou privés.



# ACOUSTICS 2012

## Influence of model parameter variability on the directivity filters of compact loudspeaker arrays

A. Mattioli Pasqual<sup>a</sup>, M. Pachebat<sup>b</sup> and P. Herzog<sup>b</sup>

<sup>a</sup>Universidade Federal de Lavras, Departamento de Engenharia, Campus Universitário,  
37200-000 Lavras, Brazil

<sup>b</sup>LMA, CNRS, UPR 7051, Aix-Marseille Univ, Centrale Marseille, 13402 Marseille, France  
ampasqual@gmail.com

Sound directivity control is made possible by a compact array of independently driven loudspeakers. Recently, a control system for such a multi-channel source based on its acoustic radiation modes has been proposed. These modes form an orthogonal set of velocity patterns on the source surface, and emerge from the eigendecomposition of a free-field radiation operator that depends on frequency. Since the diaphragm velocities are driven by electrical signals, each directivity filter is a set of voltages yielding a radiation mode. Moreover, these filters must take into account the acoustic coupling between the transducers if they interact inside a hollow cabinet. Usually, nominally identical drivers are distributed over a spherical frame in the shape of a Platonic solid, which leads to frequency-independent radiation modes. Furthermore, if the individual drivers possess identical electromechanical features, the directivity filters are frequency independent too. However, the electromechanical parameters of commercial loudspeakers might present a significant deviation from their nominal values due to their manufacturing process. This work discusses the effects of electromechanical parameter variability on the frequency independence of the directivity filters of Platonic solid loudspeakers. As an example, a dodecahedral loudspeaker array, whose parameters of the individual drivers are experimentally characterized, is investigated.

## 1 Introduction

A compact multichannel source made up of loudspeakers operating at the same frequency range can be used to control the directivity pattern of the sound field it radiates, which is of interest in 3D sound reproduction [1] and active control of sound [2; 3]. Usually, nominally identical transducers are distributed over a sphere-like frame according to the regular geometry of a Platonic solid in order to obtain a highly symmetrical configuration [4–7]. Besides, these compact spherical loudspeaker arrays are commonly provided with a set of preprogrammed spatial filters that lead to far-field directivities corresponding to a number of basic radiation patterns, such as the spherical harmonics [4–6] and, more recently, the acoustic radiation modes (ARMs) [8; 9]. Then, different directivities can be obtained by adjusting the gains of the spatial filters.

The ARMs present some advantages over the spherical harmonics, as described in Ref. [9], and form an orthogonal set of vibration patterns on the source surface. For a general radiator, the ARMs depend on frequency [10], but it has been demonstrated that they are frequency independent as far as Platonic loudspeakers are concerned [9], which greatly simplifies the spatial filters. However, each directivity filter is a set of voltages yielding a radiation mode. Moreover, these filters must take into account the acoustic coupling between the transducers if they interact inside a hollow cabinet. Therefore, even if the ARMs do not depend on frequency, the spatial filters might do. In fact, if the individual drivers possess identical electromechanical features, the directivity filters are frequency independent too whether or not the transducers are provided with their own sealed cavities [9]. However, the electromechanical parameters of commercial loudspeakers might present a significant deviation from their nominal values due to their manufacturing process.

Although the modeling, design and control of Platonic loudspeakers have been a research topic since the 1990's, directivity controlled sound sources are not commercially available yet. An issue that remains unexplored is the effects of the drivers variability on the control of compact loudspeaker arrays. This is dealt with in this work, which discusses the effects of electromechanical parameter variability on the frequency independence of the ARM-based directivity filters of Platonic solid loudspeakers. As an example, a dodecahedral loudspeaker array, whose parameters of the individual drivers are experimentally characterized, is investigated.

## 2 Theoretical background

Throughout this paper, a harmonic time dependence of the form  $e^{-j\omega t}$  is assumed, where  $j \equiv \sqrt{-1}$ ,  $\omega$  is the angular frequency, and  $t$  is the time. In addition, lower case bold letters indicate vectors, while upper case bold letters indicate matrices.

### 2.1 Acoustic radiation modes

This subsection deals with the modal representation of the free-field sound radiation from an almost spherical array of identical axisymmetric radiators, such as the tetrahedral array made up of  $L = 4$  radiators depicted in Fig. 1, where the black arrows indicate the symmetry axis of the individual radiators, the gray arrows constitute the global Cartesian coordinates system, and the spherical grid represents a rigid sphere on which the radiators are mounted. In addition, we let  $\mathbb{S}_l$  be the vibrating surface of the  $l$ th radiator, so that  $\mathbb{S} = \mathbb{S}_1 \cup \mathbb{S}_2 \cup \dots \cup \mathbb{S}_L$  is the net vibrating surface of the source.

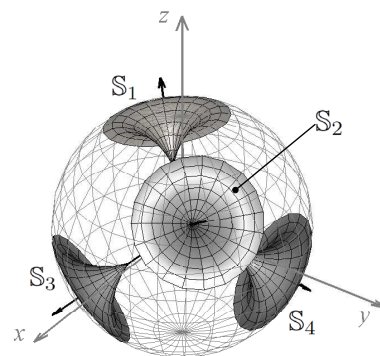


Figure 1: Compact spherical array made up of four identical axisymmetric radiators in a tetrahedral configuration.

For a vibrating structure with  $L$  degrees of freedom, the ARMs form a set of  $L$  real orthogonal vectors that span the subspace of the achievable velocity patterns over the body surface. They can be obtained through an eigenvalue analysis of a radiation operator: the eigenvectors give the ARMs and the eigenvalues their radiation efficiencies. The radiation efficiency,  $\sigma$ , of an arbitrary radiator is commonly defined as [10]

$$\sigma(\omega) \equiv \frac{\Pi(\omega)}{\rho c S \langle |v_n(\mathbf{x}_s, \omega)|^2 \rangle}, \quad (1)$$

where  $\Pi$  is the radiated sound power,  $\rho$  is the medium density,  $c$  is the sound speed,  $S$  is the surface area of  $\mathbb{S}$ ,  $\mathbf{v}_n$  is the velocity normal to  $\mathbb{S}$ ,  $\mathbf{x}_s \in \mathbb{S}$  is a point on the vibrating surface of the body, and  $\langle \cdot \rangle \equiv (2S)^{-1} \int_{\mathbb{S}} (\cdot) d\mathbf{x}_s$  is a spatial mean operator.

Let  $\mathbf{u}(\omega)$  be a column vector containing the velocity amplitude coefficients of the  $L$  degrees of freedom of a vibrating body, so that the sound power it radiates can be written as [10]

$$\Pi(\omega) = \mathbf{u}(\omega)^H \mathbf{W}(\omega) \mathbf{u}(\omega), \quad (2)$$

where the superscript H indicates the complex conjugate transpose and  $\mathbf{W}$  is an  $L \times L$  matrix that couples the sound power radiated by the elements of  $\mathbf{u}$ . From now on, the frequency dependence of  $\mathbf{u}$ ,  $\mathbf{W}$  and  $\sigma$  will be omitted for the sake of notation convenience.

As far as a compact spherical radiator array is concerned, the  $l$ th element of  $\mathbf{u}$  is a reference velocity taken at a given point in  $\mathbb{S}_l$ . This does not mean that only piston-like motion is considered here, but that there are only  $L$  controllable degrees of freedom. Besides, if the individual radiators are geometrically identical and do not overlap, it can be shown that  $\mathbf{W}$  is a real symmetric matrix and that [9]

$$\sigma(\mathbf{u}) \propto \frac{\mathbf{u}^H \mathbf{W} \mathbf{u}}{\mathbf{u}^H \mathbf{u}}. \quad (3)$$

Let  $\psi$  and  $\lambda$  be, respectively, a given but arbitrary eigenvector and eigenvalue of  $\mathbf{W}$ . Since  $\sigma$  is in the form of the Rayleigh quotient in Eq. (3),  $\psi$  is a saddle point of  $\sigma(\mathbf{u})$  and  $\sigma(\psi) \propto \lambda$ . Therefore, the solution of the eigenvalue problem

$$\mathbf{W}\psi = \lambda\psi \quad (4)$$

leads to a set of  $L$  real orthogonal eigenvectors  $\psi_1, \psi_2, \dots, \psi_L$  corresponding to real eigenvalues  $\lambda_1, \lambda_2, \dots, \lambda_L$ , where  $\lambda_l \propto \sigma(\psi_l)$ . These eigenvectors are the ARMs, which span a finite dimension subspace on which any vibration pattern the array is able to produce can be projected with no approximation error. Therefore, if  $\Psi$  is an  $L \times L$  modal matrix whose columns contain the radiation modes,  $\psi_l$ , one may write

$$\mathbf{u} = \Psi \mathbf{c}, \quad (5)$$

where  $\mathbf{c}$  is a column vector of modal contributions.

The ARMs radiate sound energy independently and allow ranking the expansion terms by their radiation efficiencies. Thus, by discarding the inefficient modes, this approach is useful in the inverse problem of determining the vibration pattern from a known acoustical field. In addition, it leads to a reduced number of active modes in sound reproduction applications because it does not make sense to drive low-efficiency ARMs. Moreover, although  $\mathbf{W}$  is frequency dependent, Pasqual and Martin [9] have demonstrated that the ARMs of the Platonic solid loudspeakers do not depend on frequency provided that the individual drivers of the array give rise to axisymmetric sound fields. The modal matrices of these arrays are explicitly given in Ref. [11]

## 2.2 Electromechanical modeling

The ARMs describe velocity patterns over the surface of a vibrating body. However, as far as loudspeaker arrays are concerned, voltages rather than velocities are controlled in practice. Hence, it is important to determine the set of voltages that leads to each ARM of the loudspeaker array, i.e.,

an appropriate transduction matrix,  $\mathbf{T}(\omega)$ , must be known, which gives the voice-coil voltages from the membrane velocities according to the equation

$$\mathbf{v}(\omega) = \mathbf{T}(\omega) \mathbf{u}(\omega), \quad (6)$$

where  $\mathbf{v}$  is a column vector containing the voltages of the  $L$  drivers of the array.

The vector  $\mathbf{v}$  is obtained from the desired ARM by letting  $\mathbf{u} = \psi$  in Eq. (6). The off-diagonal terms of  $\mathbf{T}$  take into account the internal acoustic coupling between the drivers of the array (the external coupling is of minor importance); if each driver is provided with its own sealed cavity, the off-diagonal entries are zero. In the following, in order to obtain  $\mathbf{T}$ , a lumped-parameter model of an array of electrodynamic loudspeakers mounted on a common hollow cabinet is briefly presented. For further details, see Ref. [7].

In the low-frequency range, an electrodynamic loudspeaker can be modeled as a single degree-of-freedom (SDOF) mechanical system driven by electromagnetic and acoustic forces [12]. The mass of the driver membrane assembly  $M$ , the mechanical compliance of the driver suspension  $C$  and its mechanical resistance  $R$  provide, respectively, the inertial, the energy storage and the energy dissipation elements of the SDOF system. Then, application of the Newton's second law yields

$$-j\omega M_l u_l + R_l u_l - \frac{1}{j\omega C_l} u_l = F_l^{(e)} + F_l^{(a)}, \quad (7)$$

where the subscript  $l$  refers to the  $l$ th driver of the array,  $u_l$  is its velocity,  $F_l^{(e)}$  is the electromagnetic force and  $F_l^{(a)}$  is the force acting on the inner surface of the driver membrane due to the internal acoustical load.

Now, let  $B$  be the magnetic flux density in the driver air gap and  $l_e$  the length of the voice-coil conductor in the magnetic field, so that the diaphragm movement generates an induced voltage given by  $Bl_e u$ . On the other hand, the electromagnetic force acting on the diaphragm due to the presence of an electrical current  $i$  in a magnetic field is given by  $F^{(e)} = Bl_e i$ . Hence, application of the Kirchhoff's second law leads to

$$F_l^{(e)} = \frac{(Bl_e)_l}{R_l^{(e)}} [v_l - (Bl_e)_l u_l], \quad (8)$$

where  $(Bl_e)_l$  is the force factor of the  $l$ th driver,  $R_l^{(e)}$  is the electrical resistance of its voice-coil and  $v_l$  is the voltage that feeds the  $l$ th driver.

Substitution of Eq. (8) into (7) yields

$$\left[ Z_l^{(m)} + \frac{(Bl_e)_l^2}{R_l^{(e)}} \right] u_l - F_l^{(a)} = \frac{(Bl_e)_l}{R_l^{(e)}} v_l, \quad (9)$$

where  $Z_l^{(m)} = -j\omega M_l + R_l - (j\omega C_l)^{-1}$  is the mechanical impedance of the  $l$ th driver.

Now, let  $V_b$  be the net internal volume of the cabinet. If its overall dimensions are much smaller than an acoustic wavelength and the energy dissipation is not taken into account, the enclosure behavior can be described by an acoustical compliance  $C_b = V_b / \rho c^2$  [13]. Therefore, one has [7]

$$F_l^{(a)} = A_l \sum_{r=1}^L \frac{\rho c^2}{j\omega V_b} A_r u_r, \quad (10)$$

where  $A_l$  is the net surface area of the  $l$ th driver.

Finally, it follows by inspection of Eqs. (6), (9) and (10) that the entries of  $\mathbf{T}$  are

$$T_{ll'} = \left\{ \left[ Z_l^{(m)} + \frac{(Bl_e)_l^2}{R_l^{(e)}} \right] \delta_{ll'} - \frac{\rho c^2}{j\omega V_b} A_l A_{l'} \right\} \frac{R_l^{(e)}}{(Bl_e)_l}, \quad (11)$$

where  $\delta_{ll'}$  is the Kronecker delta.

### 3 Model parameter variability

In the deterministic model described in Sec. 2.2, each driver of the loudspeaker array possesses 6 independent parameters, namely,  $M$ ,  $R$ ,  $C$ ,  $R^{(e)}$ ,  $Bl_e$  and  $A$ . Hence,  $6L$  independent parameters related to the individual transducers are required to obtain  $\mathbf{T}$ . Clearly, if the drivers are identical, only 6 parameters are needed. This section focuses on Platonic solid arrays made up of transducers that are only nominally identical; the model parameter variability introduced by the manufacturing process is taken into account by considering these 6 parameters as random variables with mean values  $\overline{M}$ ,  $\overline{R}$ ,  $\overline{C}$ ,  $\overline{R^{(e)}}$ ,  $\overline{Bl_e}$  and  $\overline{A}$ . These values lead to the nominal transduction matrix,  $\overline{\mathbf{T}}$ , whose entries are

$$\overline{T}_{ll'} = \left\{ \left[ \overline{Z}^{(m)} + \frac{(\overline{Bl_e})^2}{\overline{R^{(e)}}} \right] \delta_{ll'} - \frac{\rho c^2}{j\omega V_b} \overline{A}^2 \right\} \frac{\overline{R^{(e)}}}{\overline{Bl_e}}, \quad (12)$$

where  $\overline{Z}^{(m)} = -j\omega\overline{M} + \overline{R} - (j\omega\overline{C})^{-1}$ .

As said before, the ARMs of the Platonic loudspeakers do not depend on  $\omega$ . Moreover, they are eigenvectors of  $\overline{\mathbf{T}}$  [9]. Thus, the set of nominal voltages  $\overline{\mathbf{v}}_l$  that leads to the  $l$ th ARM is

$$\overline{\mathbf{v}}_l(\omega) = \overline{\mathbf{T}}(\omega) \boldsymbol{\psi}_l = \mu_l(\omega) \boldsymbol{\psi}_l, \quad (13)$$

where  $\mu_l$  is the  $l$ th eigenvalue of  $\overline{\mathbf{T}}$ .

If the model parameter variability is taken into account, the set of voltages  $\mathbf{v}_l$  that leads to  $\boldsymbol{\psi}_l$  is

$$\mathbf{v}_l(\omega) = \mathbf{T}(\omega) \boldsymbol{\psi}_l, \quad (14)$$

where  $\mathbf{T}$  now takes into account the deviation of the electromechanical parameters from their nominal values.

The error due to the transducers variability can be evaluated by the difference between the ARMs and the velocity patterns produced by  $\overline{\mathbf{v}}_l$  when the drivers variability is taken into consideration; these patterns are given by  $\mathbf{T}^{-1}\overline{\mathbf{v}}_l$ . Such a difference can be evaluated by

$$\epsilon_l(\omega) = \frac{\|\mathbf{T}^{-1}(\omega)\overline{\mathbf{v}}_l(\omega) - \boldsymbol{\psi}_l\|_2}{\|\boldsymbol{\psi}_l\|_2}. \quad (15)$$

Substitution of Eq. (13) into (15) yields

$$\epsilon_l(\omega) = \frac{\|\mathbf{T}^{-1}(\omega)\mu_l(\omega) - \mathbf{I}\|_2 \|\boldsymbol{\psi}_l\|_2}{\|\boldsymbol{\psi}_l\|_2}. \quad (16)$$

It is worth noting that  $\overline{\mathbf{T}}$  possesses only two distinct eigenvalues ( $\mu_1$  and  $\mu_{2-L}$ ) regardless of  $L$  [9], which simplifies the computation of  $\epsilon$ .

Finally, inspection of Eqs. (11) and (16) shows that  $\epsilon_l$  depends non-linearly on the values of  $6L$  independent parameters. In addition, the influence of each parameter on  $\epsilon_l$  depends on the values of other parameters. This complicates the uncertainty propagation analysis, and thus a Monte Carlo method is used in this work, which will be presented in the next section.

## 4 Case study: a dodecahedral array

In order to illustrate the ideas presented throughout the paper, this section investigates a real compact array of twelve transducers distributed on a spherical frame according to the dodecahedron geometry. Figure 2 shows this dodecahedral array, which has been designed and built by the authors.

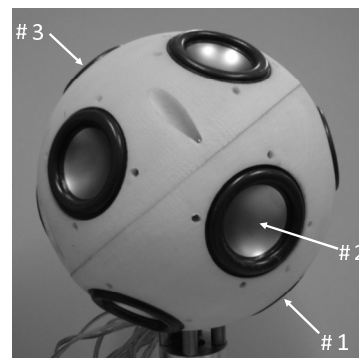


Figure 2: Spherical array prototype with  $L = 12$  independent transducers mounted on a sphere with radius  $r_e = 0.075$  m.

The exterior and interior radius of this loudspeaker array are  $r_e = 0.075$  m and  $r_i = 0.066$  m, respectively; and it is made up of twelve Aurasound<sup>®</sup> NSW2-326-8A drivers (nominal diameter: 0.051 m). In order to obtain a first statistical representation of the electromechanical parameters of the individual drivers, 16 samples of the Aurasound<sup>®</sup> NSW2-326-8A drivers have been considered. For each individual transducer, the six parameters mentioned before ( $M$ ,  $R$ ,  $C$ ,  $R^{(e)}$ ,  $Bl_e$  and  $A$ ) have been estimated from a set of electrical impedance measurements. Then, their mean values and standard deviations have been derived from the results obtained for the 16 drivers. These are shown in Table 1, as well as the Relative Standard Deviation (RSD) expressed in percentages. For further details on the parameter estimation method and on the spherical array design, see Ref. [7]. It is worth noting that, since only 16 samples have been considered, the statistical descriptors given in Table 1 are provided for guidance and illustrative purposes only.

Table 1: Estimated model parameters.

Parameter	Mean value	Standard deviation	RSD (%)
$M$ (kg)	$1.09 \times 10^{-3}$	$0.05 \times 10^{-3}$	4.6
$R$ (N.s/m)	0.2760	0.0256	9.3
$C$ (m/N)	$4.780 \times 10^{-4}$	$0.545 \times 10^{-4}$	11.4
$R^{(e)}$ ( $\Omega$ )	6.32	0.10	1.6
$Bl_e$ (T.m)	3.15	0.11	3.5
$A$ (m <sup>2</sup> )	$12.06 \times 10^{-4}$	$0.44 \times 10^{-4}$	3.7

Assuming a normal distribution for each of the parameters in Table 1, a Monte Carlo simulation can be used to obtain a statistical description of  $\epsilon$ . The procedure used in this work is as follows:

1. To evaluate  $\overline{\mathbf{T}}$  from Eq. (12) and the mean values in

Table 1;

2. To evaluate  $\mu$ , which are the eigenvalues of  $\bar{\mathbf{T}}$ ;
3. To obtain twelve values for each one of the six parameters by using a pseudorandom number generator together with the values given in Table 1;
4. To evaluate  $\mathbf{T}$  from Eq. (11) by using the  $6 \times 12 = 72$  values obtained in step 3;
5. To calculate  $\epsilon$  from Eq. (16) and to record the results;
6. To repeat steps 3 to 5 a large number of times;
7. To obtain a statistical description of  $\epsilon$  from the recorded data.

Some results obtained by using this procedure with 5000 samples in the Monte Carlo simulation are presented below.

Figure 3 shows the mean value of  $\epsilon$ ,  $\bar{\epsilon}$ , as a function of frequency for the twelve ARMs of the dodecahedral loudspeaker array. It can be noticed that  $\bar{\epsilon}$  is larger in the low-frequency range and stabilizes at the value 0.06 approximately as frequency increases, regardless of the ARM considered. In fact, as indicated in Table 1, the relative standard deviations of  $C$  and  $M$  are 11.4% and 4.6%, respectively. Because  $C$  possesses a larger variability than  $M$ ,  $\bar{\epsilon}$  is larger in the compliance-dominated frequency range, i.e., at the low frequencies, as Figure 3 reveals. Besides, the ARM # 1 has a larger  $\bar{\epsilon}$  than the ARMs # 2-12 due to the acoustic interaction between the drivers inside the hollow spherical cabinet, which is more pronounced for the ARM # 1 (transducers in phase), mainly at low frequencies. Inspection of Figure 3 also reveals that  $\bar{\epsilon}$  depends significantly on frequency from 200 Hz to 500 Hz approximately, so that the directivity filters cannot be considered as frequency independent in this frequency range.

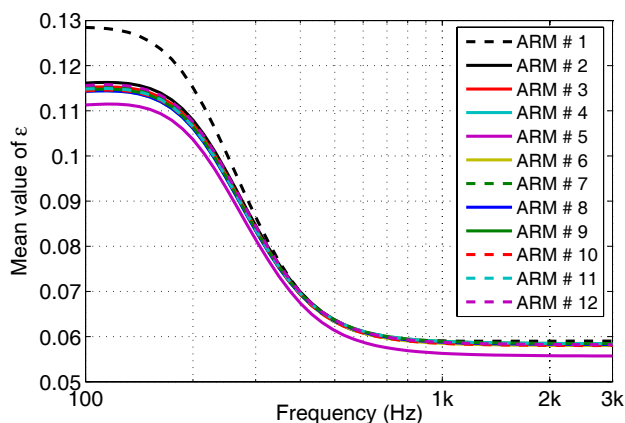


Figure 3: Mean value of  $\epsilon$  for the twelve ARMs of the dodecahedral loudspeaker array.

Figures 4 to 7 show the boxplots for  $\epsilon$  corresponding to the ARMs # 1, 3, 5 and 11, respectively. For the sake of clarity, the data are given for only ten frequency values, which are equally spaced from 100 Hz to 1 kHz. The boxplot is a simple way to describe graphically the statistical properties of a random variable; on each box, the red mark is the median, the blue edges of the box are the lower and upper quartiles, and the whiskers extend to the most extreme data points not considered outliers.

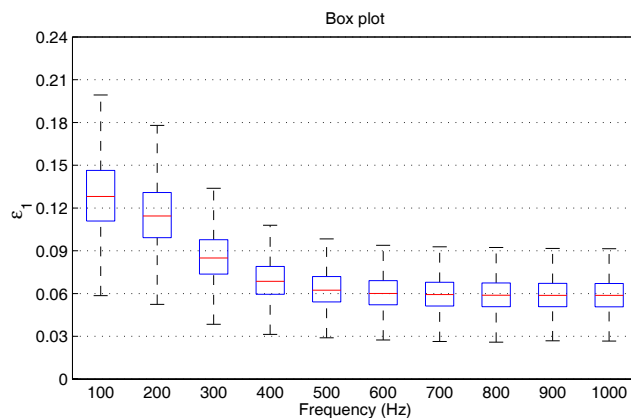


Figure 4: Boxplot for  $\epsilon$  corresponding to the ARM # 1.

It can be noticed that  $\epsilon_1$  presents a smaller variability in the whole frequency range compared with  $\epsilon_3$ ,  $\epsilon_5$  and  $\epsilon_{11}$ . In addition, the variability is larger at low frequencies; in the high-frequency range,  $\epsilon$  would be hardly larger than 0.12, which is the upper value in the boxplot of  $\epsilon_5$  (Figure 6). These results, together with those presented in Figure 3, indicate that the effects of the electromechanical parameter variability on the spatial filters might be relevant, especially in the low-frequency range. Therefore, one must be careful in selecting transducers for a directivity controlled sound source.

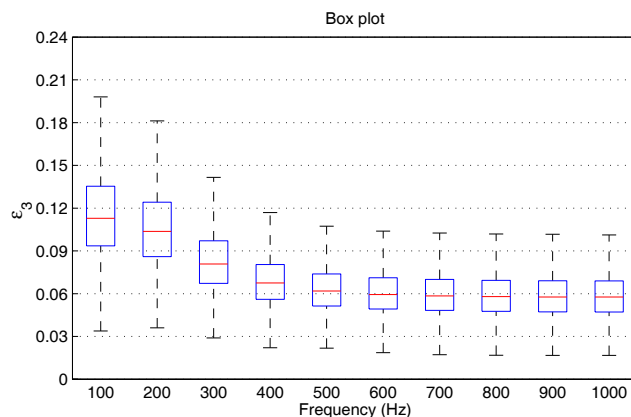


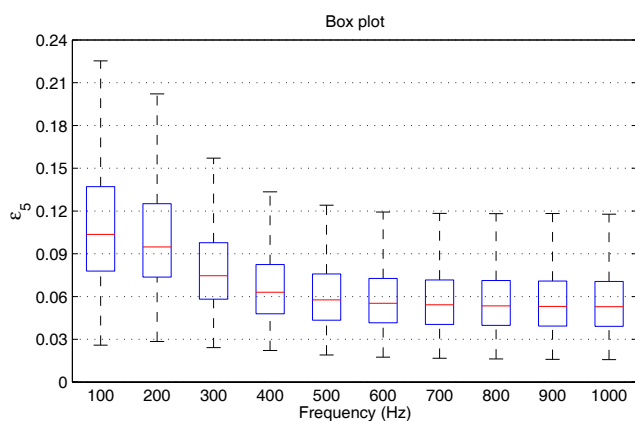
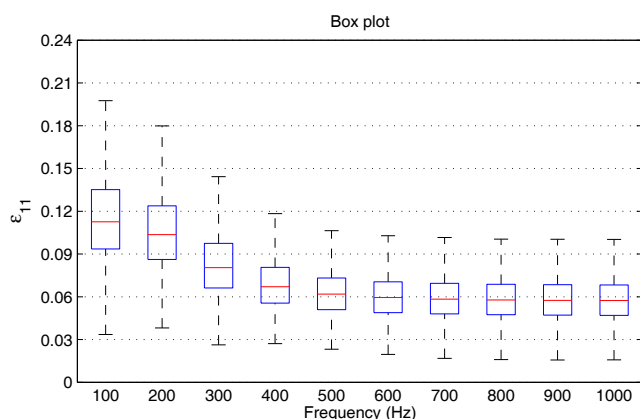
Figure 5: Boxplot for  $\epsilon$  corresponding to the ARM # 3.

## 5 Conclusion

Platonic solid loudspeakers present the advantage of having frequency-independent radiation modes. In addition, if the individual drivers of the array possess identical electromechanical features, the ARM-based directivity filters do not depend on frequency either. However, the electromechanical parameters of commercial driver units might present a significant deviation from their nominal values due to the manufacturing process, which might lead to frequency-dependent directivity filters.

This paper investigated the effects of the above-mentioned parameter variability on the directivity filters of Platonic loudspeakers. As a case study, a real dodecahedral array was considered. Monte Carlo simulation results indicated that the manufacturing variability of loudspeaker units might lead to



Figure 6: Boxplot for  $\epsilon$  corresponding to the ARM # 5.Figure 7: Boxplot for  $\epsilon$  corresponding to the ARM # 11.

frequency-dependent directivity filters, especially in the low- and medium-frequency ranges due to the large variability of the suspension compliance. Thus, one must consider using transducers built with high manufacturing tolerances in compact loudspeaker arrays for directivity control.

## Acknowledgments

The authors wish to acknowledge the financial support of the *Centre National de la Recherche Scientifique* (CNRS, France).

## References

- [1] O. Warusfel, P. Derogis, and R. Caussé, "Radiation synthesis with digitally controlled loudspeakers," in *Proceedings of the 103rd Audio Engineering Society Convention*, (New York), pp. 1–11, Sept. 1997. Paper number 4577.
- [2] B. Rafaely, "Spherical loudspeaker array for local active control of sound," *J. Acoust. Soc. Am.*, vol. 125, pp. 3006–3017, May 2009.
- [3] T. Peleg and B. Rafaely, "Investigation of spherical loudspeaker arrays for local active control of sound," *J. Acoust. Soc. Am.*, vol. 130, pp. 1926–1935, Oct. 2011.
- [4] P. Kassakian and D. Wessel, "Characterization of spherical loudspeaker arrays," in *Proceedings of the 117th Audio Engineering Society Convention*, (San Francisco, CA, USA), pp. 1–15, Oct. 2004. Paper number 6283.
- [5] F. Zotter, H. Pomberger, and A. Schmeder, "Efficient directivity pattern control for spherical loudspeaker arrays," in *Proceedings of the 2nd ASA-EAA Joint Conference*, (Paris), pp. 4229–4234, June 2008.
- [6] M. Pollow and G. K. Behler, "Variable directivity for Platonic sound sources based on spherical harmonics optimization," *Acta Acust. Acust.*, vol. 95, pp. 1082–1092, Nov. 2009.
- [7] A. M. Pasqual, P. Herzog, and J. R. F. Arruda, "Theoretical and experimental analysis of the electromechanical behavior of a compact spherical loudspeaker array for directivity control," *J. Acoust. Soc. Am.*, vol. 128, pp. 3478–3488, Dec. 2010.
- [8] A. M. Pasqual, J. R. F. Arruda, and P. Herzog, "Application of acoustic radiation modes in the directivity control by a spherical loudspeaker array," *Acta Acust. Acust.*, vol. 96, pp. 32–42, Jan. 2010.
- [9] A. M. Pasqual and V. Martin, "On the acoustic radiation modes of compact regular polyhedral arrays of independent loudspeakers," *J. Acoust. Soc. Am.*, vol. 130, pp. 1325–1336, Sept. 2011.
- [10] K. A. Cunefare, M. N. Currey, M. E. Johnson, and S. J. Elliott, "The radiation efficiency grouping of free-space acoustic radiation modes," *J. Acoust. Soc. Am.*, vol. 109, pp. 203–215, Jan. 2001.
- [11] A. M. Pasqual, *Sound directivity control in a 3-D space by a compact spherical loudspeaker array*. PhD dissertation, State University of Campinas, Faculty of Mechanical Engineering, Campinas/SP, Brazil, 2010. available at <http://tel.archives-ouvertes.fr/> (last viewed 1/26/12).
- [12] M. Rossi, *Audio*. Lausanne: Presses Polytechniques et Universitaires Romandes, 2007.
- [13] A. D. Pierce, *Acoustics: An Introduction to Its Physical Principles and Applications*, ch. 7, pp. 313–370. Melville, NY: Acoustical Society of America, 1994.